step being determined by the time to reach a fixed neutron count on a monitor placed between the source and the sample. The scanning interval was 2.0, 1.5, 2.1, 2.9, and 4.0° for θ = 0, 15, 30, 40, and 56°, respectively, and interpolated for the θ values in between. The intensities and their standard deviations were evaluatd by a peak profile analysis using the Lehmann and Larsen algorithm.[40] Intensities were corrected for the effects of absorption by assuming the crystal to be spherical ($\mu R = 0.195$). A total of 1503 reflections [$+h,+k,+l$] were measured in the range $6.68 < \theta < 57.05°$ and were averaged to give 727 independent reflections ($R_{av} = 0.014$),[41] and these were used in the subsequent refinement of the structure.

Structure Refinement. Atomic positional parameters taken from an earlier X-ray experiment were used as a starting point for the refinement with the neutron diffraction data. Refinement was by full-matrix least squares where the quantity minimized was $\sum w(|F_0| - |F_c|)^2$. Refinement converged at $R = 0.027$ and $R_w = 0.022$[42] ($w = 1/\sigma(F_0)^2$) with 79 parameters. Scattering lengths were taken from ref 43. In the final refinement cycle the mean shift to error ratio was less than 10^{-5}. Table VI gives the final atomic fractional coordinates and the thermal parameters. A list of observed and calculated structure factors has been deposited as supplementary material.

Acknowledgment. R.G. and C.K. are most grateful to Dr. M. Rubach for supplying the crystals. F.M. and X.Z. wish to thank Dr. P. J. Jolly and Dr. R. Benn for communicating and discussing recent experimental results. Part of this work was supported by the Deutsche Forschungsgemeinschaft.

Registry No. *trans*-Bis(η^3-allyl)nickel, 75110-62-2.

Supplementary Material Available: Crystal data, a table (Table VI) of positional and thermal parameters, and a list of observed and calculated structure factors for the neutron diffraction experiment (5 pages). Ordering information is given on any current masthead page.

---

(40) Lehmann, M. S.; Larsen, F. K. *Acta Crystallogr., Sect. A* 1974, *A30*, 580.

(41) R_{av} defined as $\sum|\langle I\rangle - I|/\sum|I|$, where $\langle I\rangle$ is the local average for equivalent reflections.

(42) $R = \sum(|F_0| - |F_c|)/\sum|F_0|$. $R_w = (\sum w(|F_0| - |F_c|)^2/\sum w|F_0|^2)^{1/2}$.

(43) The following scattering amplitudes were used: H, −0.374, C, 0.66, and Ni, 1.03 × 10^{-12} cm. Bacon, G. E. "Neutron Diffraction"; Oxford University Press: Oxford, 1962.

σ/π Interactions in Alkynyltin(IV) Compounds Studied by UV Photoelectron Spectroscopy and Pseudopotential "ab Initio" Calculations

Carla Cauletti* and Claudio Furlani

Dipartimento di Chimica, Università "La Sapienza" di Roma, 00185 Roma, Italy

Gaetano Granozzi

Istituto di Chimica Generale ed Inorganica, Università di Padova, Padova, Italy

Angelika Sebald and Bernd Wrackmeyer

Institut für Anorganische Chemie, Universität München, München, Federal Republic of Germany

Received April 11, 1984

Joint analysis of gas-phase UV photoelectron spectra (UPS) and pseudopotential "ab initio" calculations was used to gain insight into the nature and the mechanism of the interactions between the $\pi_{C\equiv C}$ and σ_{Sn-C} orbitals in a series of alkyltin acetylides. The results clearly indicate that the σ/π conjugation is quite extensive along the whole series and that the mechanism is critically controlled by the substituents at both the tin and the alkynyl moiety. Good agreement between the experimental ionization energies and the eigenvalues calculated by the pseudopotential "ab initio" model indicates that this method is suitable for a nonempirical description of the electronic structure of a molecule containing heavy atoms.

Introduction

σ/π interactions (where σ and π are referred to local bond symmetry) have been the subject of several investigations by means of gas-phase UV photoelectron spectroscopy (UPS), mainly in some alkyl-substituted acetylenic compounds.[1-6] In this class of molecules the mechanism of the σ/π conjugation is of a relatively simple nature, since the orbital energy of the σ orbitals is always lower than that of the $\pi_{C\equiv C}$ orbitals, and the effect of the interaction is therefore always destabilizing for the π levels. The same occurs in the case of silyl-substituted acetylenes, also studied by UPS.[2] The extention of these results to alkyltin derivatives of alkynes is not straightforward and extrapolation would not be warranted: in fact in these molecules the orbitals involved in the σ/π conjugation, that

---

(1) Brogli, F.; Heilbronner, E.; Hornung, V.; Kloster-Jensen, E. *Helv. Chim. Acta* 1973, *56*, 2171.

(2) Ensslin, W.; Bock, H.; Becker, G. *J. Am. Chem. Soc.* 1974, *96*, 2757.

(3) Brogli, F.; Heilbronner, E.; Wirz, J.; Kloster-Jensen, E.; Bergmann, R. G.; Vollhardt, K. P. C.; Ashe III, A. J. *Helv. Chim. Acta* 1975, *58*, 2620.

(4) Carlier, P.; Dubois, J. E.; Masclet, P.; Mouvier, G. *J. Electron Spectrosc. Relat. Phenom.* 1975, *7*, 55.

(5) Bieri, G.; Heilbronner, E.; Kloster-Jensen, E.; Maier, J. P. *Phys. Scr.* 1977, *16*, 202.

(6) Bieri, G.; Burger, F.; Heilbronner, E.; Maier, J. P. *Helv. Chim. Acta* 1977, *60*, 2213.

0276-7333/85/2304-0290$01.50/0 © 1985 American Chemical Society

Table I. Pseudopotential Parameters for the Tin and Carbon Atoms

atom	l	α	n_i	a_i
Sn	0	1.357 58	0	27.792 30
			2	−9.754 05
	1	0.604 21	0	6.215 82
			2	−1.265 69
C	0	5.330 46	−1	1.369 25
			0	21.035 11
	1	14.061 16	0	−6.052 01

is the $\pi_{C\equiv C}$ and the σ_{Sn-C} orbitals, are in most cases closer in energy than the corresponding orbitals in the alkyl- and silyl-substituted acetylenes, so that a more extensive σ/π mixing may occur. A further and more significant aspect, peculiar to σ/π interaction in the alkyltin acetylides, is that the relative ordering of the σ and π energy levels of the two moieties is more difficult to predict than in the simple acetylenes, since it depends critically on the number and type of alkyltin substituents, which exert an inductive electron-releasing effect on the alkynyl fragments.

All these reasons prompted us to investigate by UPS a series of alkyltin alkynes, already studied by some of us (A.S. and B.W.) by NMR.[7,8]

Examples of UPS studies on the σ/π conjugation in alkyltin compounds are not numerous; they deal mainly with some allyl- and vinylstannanes[9-11] where the electronic situation is, however, quite different from the present case. The investigated compounds were **1**–**5**.

$Et_3SnC{\equiv}CH$ **1**

$Me_3SnC{\equiv}CMe$ **2**

$Me_3SnC{\equiv}CSnMe_3$ **3**

$Me_3SnC{\equiv}CC{\equiv}CSnMe_3$ **4**

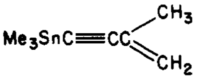

$Me_3SnC{\equiv}CC(CH_3){=}CH_2$

5

The interpretation of the UP spectra was based on fragment analysis, starting from literature data on parent molecules. Furthermore, we used the pseudopotential method in order to calculate at the "ab initio" accuracy level the ground-state electronic structure of some representative molecules. The theoretical results will allow a quantitative evaluation of σ/π interactions.

Experimental Section

Preparations. The compounds studied were prepared by literature methods.[12-14] Purity was checked by the absence of spurious signals in the ^1H and ^{13}C NMR spectra.

UP Spectra. He I and He II gas-phase photoelectron spectra were recorded on a Perkin-Elmer PS 18 spectrometer modified with a hollow cathode discharge lamp (Helectros Developments). $Me_3SnC{\equiv}CSnMe_3$ and $Me_3SnC{\equiv}CC{\equiv}CSnMe_3$, which are solid at room temperature, were heated (at ca. 30 and 75 °C, respectively) to get reasonably intense spectra. Calibration was performed by reference to the peaks of standard gases (Ar, CH_3I) allowed into the ionization chamber and the peak of the He 1_s^{-1} self-ionization.

Table II. Orbital Exponents and Coefficients of the 3-1 G Split Gaussian Basis Sets

atom	orbital	exponent	coeff
Sn	s	1.740 37	0.252 61
		1.074 62	−0.603 34
		0.187 35	0.692 62
		0.072 33	1.0
	p	1.511 70	0.068 98
		1.073 10	−0.119 59
		0.180 22	0.589 89
		0.061 09	1.0
C	s	2.382 01	−0.242 14
		1.443 06	0.185 26
		0.405 85	0.591 28
		0.138 42	1.0
	p	8.609 57	0.043 65
		1.943 55	0.209 50
		0.542 80	0.502 76
		0.152 50	1.0

Table III. UPS Ionization Energies and Assignments for Alkynyltin(IV) Compounds

compound	band label	IE, eV	assignt
$Et_3SnC{\equiv}CH$	A	9.00	$e(\sigma/\pi)$
	B	10.21	$e(\sigma/\pi)$
	C	10.73	$a_1(\sigma)$
$Me_3SnC{\equiv}CMe$	A	9.23	$e(\pi)$
	B	10.12	$e(\sigma)$
	C	11.05	$a_1(\sigma)$
$Me_3SnC{\equiv}CSnMe_3$	A	8.93	$e'(\sigma/\pi)$
	B	9.78	$e''(\sigma)$
	C	10.28	$e'(\sigma/\pi) + a_1'(\sigma)$
	D	11.60	$a_1''(\sigma)$
$Me_3SnC{\equiv}CC{\equiv}CSnMe_3$	A	8.87	$e'(\sigma/\pi)$
	B	9.67	$e''(\sigma/\pi)$
	C	10.69	$e'(\sigma/\pi) + a_1'(\sigma)$
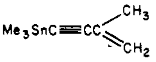 $Me_3SnC{\equiv}CC(CH_3){=}CH_2$	A	8.51	π
	B	9.17	σ/π
	C	9.82	σ
	D	10.16	σ/π
	E	10.91	$\sigma + \pi$

Calculations. The "ab initio" LCAO-MO-SCF calculations were performed with the introduction of pseudopotentials to deal with all core electrons on each atom. The formalism by Durand and co-workers[15] has been choosen, where for a given atom c the purely local operator, for each l value, has the form

$$W_{l,c}(r) = \sum_i a_i r^{n_i} \exp(-\alpha r^2)$$

The a_i, n_i, and α parameters adopted for Sn and C atoms are reported in Table I. Sn and C valence 3-1G split basis sets were optimized for each valence shell by a pseudopotential version of ATOM program[16] (Table II), whereas for H the standard Huzinaga[17] Gaussian basis set has been 3 + 1 contracted. All the molecular calculations were carried out by using the PSHONDO program.[18] The geometrical parameters adopted in the calculations were derived from the results of electron diffraction experiments,[19,20] assuming a linear array with C_{3v} and D_{3h} symmetry for $R_3SnC{\equiv}CH$ and $Me_3SnC{\equiv}CSnMe_3$, respectively.

---

(7) Sebald, A.; Wrackmeyer, B. *Spectrochim. Acta, Part A* **1981**, *37A*, 365.

(8) (a) Wrackmeyer, B. *J. Organomet. Chem.* **1978**, *145*, 183. (b) Wrackmeyer, B. *J. Organomet. Chem.* **1979**, *166*, 353. (c) Hölzl, F.; Wrackmeyer, B. *J. Organomet. Chem.* **1979**, *179*, 397. (d) Wrackmeyer, B. *J. Magn. Reson.* **1981**, *42*, 287.

(9) Schweig, A.; Weidner, U.; Manuel, G. *J. Organomet. Chem.* **1973**, *54*, 145.

(10) Brown, R. S.; Eaton, D. F.; Hosomi, A.; Traylor, T. G.; Wright, J. M. *J. Organomet. Chem.* **1974**, *66*, 249.

(11) Novak, I.; Cvitas, T.; Klasinc, L. *J. Organomet. Chem.* **1981**, *220*, 145.

(12) Brandsma, L. "Preparative Acetylenic Chemistry"; Elsevier: Amsterdam, 1971.

(13) Ben-Efraim, D. A. "The Chemistry of the Carbon-Carbon Triple Bound"; Patai, S., Ed.; Wiley: New York, 1978.

(14) Davidson, W. E.; Henry, M. C. *Chem. Rev.* **1967**, *67*, 73.

(15) Barthelat, J. C.; Durand, P.; Serafini, A. *Mol. Phys.* **1977**, *33*, 159.

(16) Roos, B.; Salez, C.; Veillard, A.; Clementi, E. "A general program for calculation of atomic SCF orbitals by the expansion method", Technical Report RJ 518; IBM Research, 1968.

(17) *Huzinaga*, S. *J. Chem. Phys.* **1965**, *42*, 1293.

(18) Daudey, J. P., a modified version of HONDO program (Dupuis, M.; Rys, J.; King, M. F. *QCPE* 336) including pseudopotentials.

(19) Khaikin, L. S.; Novikov, V. P.; Vilkov, L. V.; Zavgorodnii, V. S.; Petrov, A. A. *J. Mol. Struct.* (*Engl. Transl.*) **1977**, *39* 91.

(20) Khaikin, L. S.; Novikov, V. P.; Vilkov, L. V. *J. Mol. Struct.* (*Engl. Transl.*) **1977**, *42*, 129.

Table IV. Pseudopotential ab Initio Results for $Et_3SnC{\equiv}CH$[a]

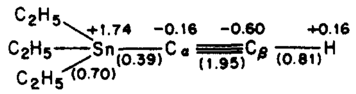

MO	eigenvalue, eV	% population Sn	C_α	C_β	H	CH_3	dominant character
$1a_1$	−28.14	3	1	1	0	95	$\sigma_{C_2H_5}$
1e	−27.64	1	0	0	0	99	$\sigma_{C_2H_5}$
$2a_1$	−27.59	1	27	61	2	9	$\sigma_{C_\alpha{\equiv}C_\beta}$
$3a_1$	−23.07	6	0	0	0	94	$\sigma_{C_2H_5}$
2e	−22.45	2	0	0	0	98	$\sigma_{C_2H_5}$
$4a_1$	−19.59	2	16	46	32	4	$\sigma_{C_\beta\text{-}H}$
$5a_1$	−17.59	18	11	6	4	61	$\sigma_{Sn\text{-}C_\alpha\text{-}C_\beta\text{-}H}$
3e	−17.01	2	0	0	0	98	$\sigma_{C_2H_5}$
$1a_2$	−15.97	0	0	0	0	100	$\sigma_{C_2H_5}$
$6a_1$	−15.89	11	31	7	3	48	$\sigma_{Sn\text{-}C_\alpha}$
4e	−15.41	0	0	0	0	100	$\sigma_{C_2H_5}$
$7a_1$	−14.05	2	0	0	0	98	$\sigma_{C_2H_5}$
5e	−13.88	0	0	0	0	100	$\sigma_{C_2H_5}$
6e	−13.42	2	0	0	0	100	$\sigma_{C_2H_5}$
$2a_2$	−12.78	0	0	0	0	100	$\sigma_{C_2H_5}$
$8a_1$	−12.15 [−12.88]	18 [17]	21 [30]	4 [4]	1 [0]	56 [52]	$\sigma_{Sn\text{-}C_2H_5}$
7e	−10.91 [−11.29]	8 [13]	36 [24]	32 [19]	0 [0]	24 [63]	σ/π mixed
8e (HOMO)	−9.89 [−10.32]	10 [6]	14 [26]	18 [30]	0 [0]	58 [39]	σ/π mixed

[a] Net atomic charges and overlap populations (in parentheses) are in electrons. In brackets are reported the results for $Me_3SnC{\equiv}CH$.

Results and Discussion

Table III reports the measured ionization energies (IEs) for all of the molecules together with their proposed assignments.

We shall now discuss in detail each single case, since a general treatment is almost impossible for the reasons explained above. For all the compounds we ran both He I and He II spectra, but in most cases no significant differences in band intensity ratios were observed. This confirms the prediction of extensive σ/π mixing, i.e., delocalization of the upper filled MOs in the whole molecule. In fact, if orbitals of largely predominant σ_{Sn-C} or $\pi_{C{\equiv}C}$ character were present in a molecule, the photoionization cross sections should be different for the two groups of systems. We shall therefore show only the He I spectra in the figures.

Another experimental finding that supports the hypothesis of a significant σ/π interaction is that in no case could we find bands with the typical shape of $\pi_{C{\equiv}C}^{-1}$ ionizations (sharp with the presence of a vibrational structure).

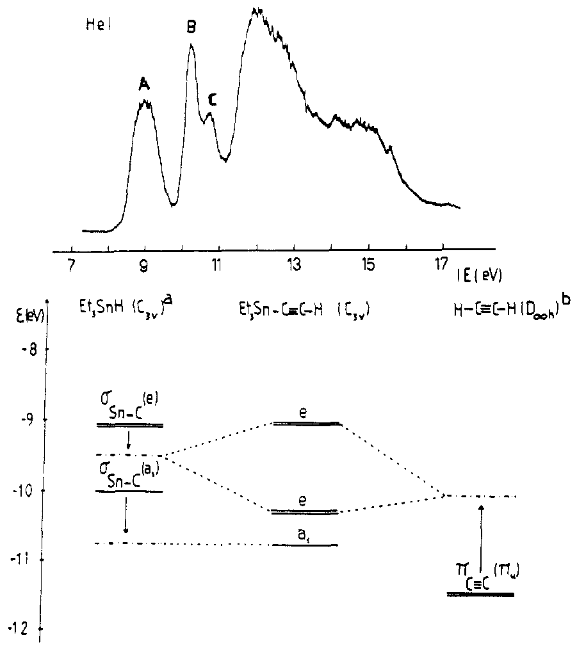

Figure 1. Gas-phase UP spectrum and correlation diagram of $Et_3SnC{\equiv}CH$. (a) IES taken from ref 21. (b) IEs taken from ref. 6.

$R_3SnC{\equiv}CR'$. The correlation diagram to discuss the UP spectrum of $Et_3SnC{\equiv}CH$ (1) starts from the parent molecules Et_3SnH and $HC{\equiv}CH$ and takes into account the mutual inductive effects of the two fragments (see Figure 1). In the figure the arrows and dotted lines indicate the direction and the estimated extent of such effects. The MO energy values used in this and in the following diagrams are taken from UPS data, assuming the validity of the Koopmans' theorem.[22] It appears from the diagram that the inductive effect exerted by the $C{\equiv}CH$ moeity on the triethyltin fragment can be estimated from the difference in IE between the $\sigma_{Sn-C}(a_1)$ in Et_3SnH and the $\sigma_{Sn-C}(a_1)$ in 1, the latter orbital being not involved in conjugation with the acetylenic orbitals. Such a shift (0.7 eV) is not observed for the σ_{Sn-C}(e) level, whose IE is almost identical in the two compounds: this fact is the result of the destabilizing interaction of σ_{Sn-C}(e) in 1 with the $\pi_{C{\equiv}C}$(e) orbital (π_u in acetylene). On the other hand, the electron-releasing effect of the Et_3Sn group on the $\pi_{C{\equiv}C}$ level should be quite strong considering the shift in IE observed on passing from $HC{\equiv}CH$ to $Me_3CC{\equiv}CH$ (11.40 and 9.92 eV, respectively).[4] Et_3Sn is certainly a better electron donor group than Me_3C, so one would expect an even larger shift to lower IE in our molecule, due to an inductive effect; however, the σ/π interaction is in the opposite direction and results in a stabilization of the e orbital of predominant $\pi_{C{\equiv}C}$ character. The results of the

---

(21) Beltram, G.; Fehlner, T. P.; Mochida, K.; Kochi, J. K. *J. Electron Spectrosc. Relat. Phenom.* **1980**, *18*, 153.

(22) Koopmans, T. C. *Physica (Amsterdam)* **1934**, *1*, 104.

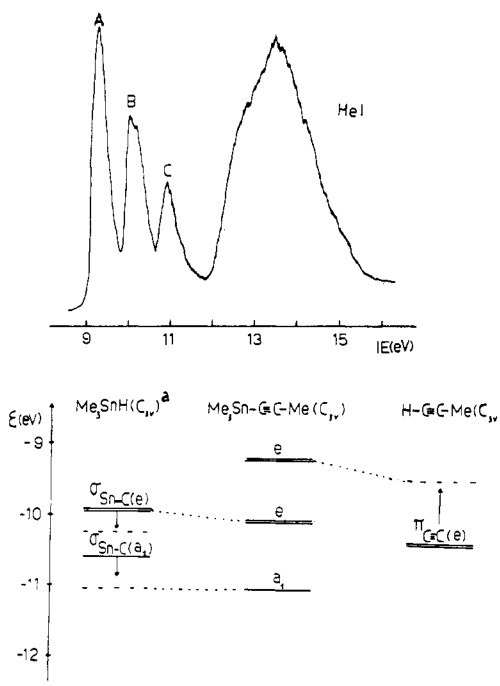

Figure 2. Gas-phase UP spectrum and correlation diagram of $Me_3SnC{\equiv}CMe$ (see a and b in Figure 1).

"ab initio" calculations are reported in Table IV where the eigenvalue and the population (%) analysis of each valence MO is reported together with relevant gross atomic charges and overlap populations obtained by applying Mulliken's method.[23] The general agreement between the computed and the experimental IEs, through Koopmans' theorem (an excellent numerical matching is obtained by multiplying the computed IEs by 0.90), supports the validity of the pseudopotential approach. The analysis of the 8e and 7e MOs confirms a strong σ/π mixing between the σ_{Sn-C}(e) and $\pi_{C\equiv C}$(e) orbitals with a predominance of $\pi_{C\equiv C}$ character for the inner one. It is noteworthy, in this respect, that a smaller bandwidth is associated with band B, which is reminiscent of the band shape of $\pi_{C\equiv C}^{-1}$ ionizations. The $8a_1$ MO is $\sigma_{Sn-C_2H_5}$ bonding but shows a relevant σ-antibonding Sn–C_α contribution. The bonding σ_{Sn-C_α} counterpart lies very low in energy ($6a_1$ at −15.89 eV), and its ionization is certainly hidden under the broad band due to the σ_{C-C} and σ_{C-H} ionizations. It is very interesting to note that according to the calculations the largest by far contribution to the Sn–C_α bonding is that of the Sn 5s AO; this allows us to predict larger ionic character for Sn–C(sp) bonds than for Sn–C(sp^3) ones coupled with lower bond strength.

In order to examine the effect of replacing the methyl by ethyl groups in the alkyltin moiety, we performed also calculations for $Me_3SnC{\equiv}CH$, which is too unstable to be measured by UPS. The results (partially reported in Table IV) clearly indicate a different σ/π mixing in the two compounds due to the fact that the stronger electron-releasing ability of ethyl groups with respect to methyl groups causes a shift in the π_{Sn-C} orbitals to higher energy. As a consequence, the difference energy sequence of the interacting σ_{Sn-C}(e) and $\pi_{C\equiv C}$(e) levels causes a change in the composition of the HOMO, which in $Me_3SnC{\equiv}CH$ shows predominant $\pi_{C\equiv C}$ character. This evidence substantiates possible changes in the relative ordering of the σ and π interacting levels induced by the R substituents, as anticipated in the introduction.

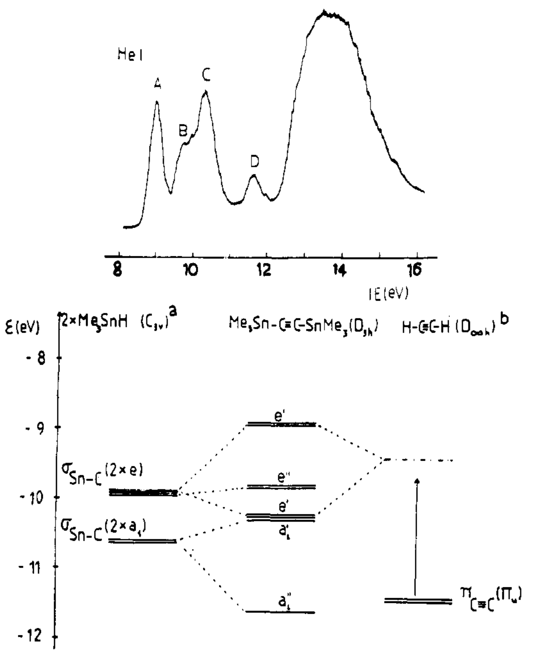

Figure 3. Gas-phase UP spectrum and correlation diagram of $Me_3SnC{\equiv}CSnMe_3$ (see a and b in Figure 1).

An even larger $\pi_{C\equiv C}$ character of the HOMO was expected in $Me_3SnC{\equiv}CMe$ (2), owing to the higher energy of this level in $MeC{\equiv}C$– fragment with respect to the $HC{\equiv}C$– fragment. In fact the observed UP spectrum and the correlation diagram (see Figure 2) live up to this expectation.

$Me_3SnC{\equiv}CSnMe_3$ (3). Figure 3 shows the spectrum and the correlation diagram for this compound. In this case the inductive effect of the –C≡C– fragment on the rest of the molecule is diluted into the two Me_3Sn groups, so that it is practically negligible. Of the four σ_{Sn-C} orbitals of e symmetry in the two Me_3SnH molecules, two (e″, assuming the D_{3h} eclipsed conformation) remain nonbonding in 3, while the other two (e′) interact with the $\pi_{C\equiv C}$ orbital. The UP spectrum shows actually a sequence of three bands in the low IE region, A, B, and C of the figure, that we assign respectively to ionizations from the e′ antibonding combination of σ_{Sn-C} and $\pi_{C\equiv C}$ levels, the e″ nonbonding orbital of pure σ_{Sn-C} character, and the e′ bonding combination of the above levels. To band C contributes also the ionization from the a_1' combination of the two Sn–C orbitals of a_1 symmetry in Me_3SnH; the a_1'' combination is related to band D.

This interpretation is fully supported by the calculation (Table V) whose results suggest for 5e′ (HOMO) and 4e′ a strong σ/π mixing with a predominance of $\pi_{C\equiv C}$ character for the former one (58%) and of σ_{Sn-C} character for the latter one. The computed energy sequence 4e′, 4e″, and 5e′ is in agreement with the experimental data, and the predicted compositions are consistent with band-shape analysis. The $5a_1'$ and $4a_1''$ MOs have σ bonding and antibonding Sn–C contributions, respectively. The computed $4a_1' - 5a_1'$ splitting supports the hypothesis that the ionization from the $5a_1'$ orbital contributes to band C.

As far as the electronic distribution is concerned, we note (Table V) a further increase in the C≡C overlap population with respect to the previously discussed molecules.

$Me_3SnC{\equiv}CC{\equiv}CSnMe_3$ (4). The UP spectrum and the correlation diagram for this compound are displayed in Figure 4.

Assuming again for this molecule a D_{3h} symmetry, both the σ_{Sn-C} (of e symmetry in Me_3SnH) and the $\pi_{C\equiv C}$ orbitals transform as e′ + e″. A significant σ/π mixing is

---

(23) Mulliken, R. S. *J. Chem. Phys.* **1955**, *23*, 1833.

Table V. Pseudopotential ab Initio Results for $Me_3SnC{\equiv}CSnMe_3$ [a]

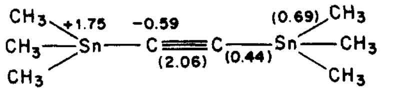

MO	eigenvalue, eV	% pop. Sn	% pop. C	% pop. CH_3	dominant character
$1a_1'$	−27.38	1	97	2	$\sigma_{C\equiv C}$
$1a_1''$	−25.64	9	0	91	σ_{CH_3}
$2a_1'$	−25.59	8	2	90	σ_{CH_3}
$1e''$	−25.03	5	0	95	σ_{CH_3}
$1e'$	−25.03	5	0	95	σ_{CH_3}
$2a_1''$	−18.27	22	61	17	$\sigma_{Sn-C\equiv}$
$3a_1'$	−16.72	34	35	31	$\sigma_{Sn-C\equiv}$
$3a_1''$	−15.23	7	0	93	σ_{CH_3}
$4a_1'$	−15.22	6	0	94	σ_{CH_3}
$2e''$	−15.10	2	0	98	σ_{CH_3}
$2e'$	−15.10	2	0	98	σ_{CH_3}
$3e'$	−14.83	1	0	99	σ_{CH_3}
$3e''$	−14.81	1	0	99	σ_{CH_3}
$1a_2'$	−14.50	0	0	100	σ_{CH_3}
$1a_2''$	−14.50	0	0	100	σ_{CH_3}
$4a_1''$	−13.37	20	24	56	σ_{Sn-CH_3}
$5a_1'$	−12.24	17	43	40	σ_{Sn-CH_3}
$4e'$	−11.35	15	38	47	σ/π mixed
$4e''$	−10.86	19	0	81	σ_{Sn-CH_3}
$5e'$ (HOMO)	−9.95	5	58	37	σ/π mixed

[a] Net atomic charges and overlap populations (in parentheses) are in electrons.

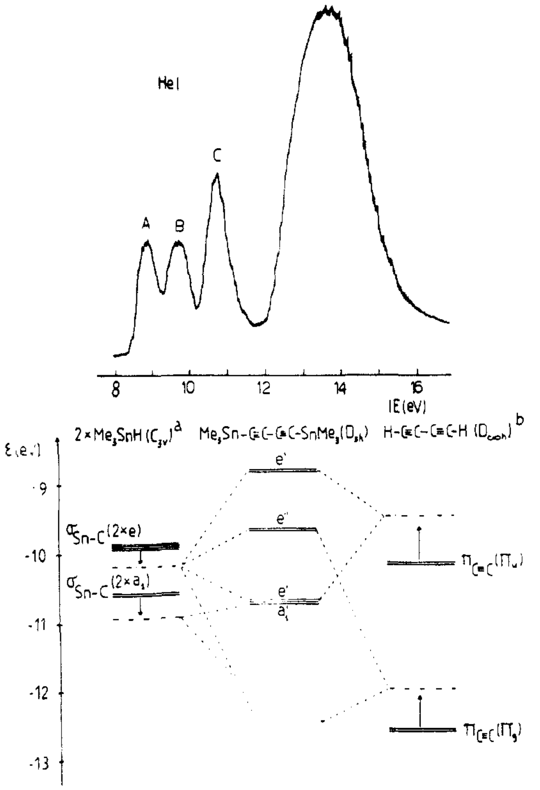

Figure 4. Gas-phase UP spectrum and correlation diagram of $Me_3SnC{\equiv}CC{\equiv}CSnMe_3$ (see a and b in Figure 1).

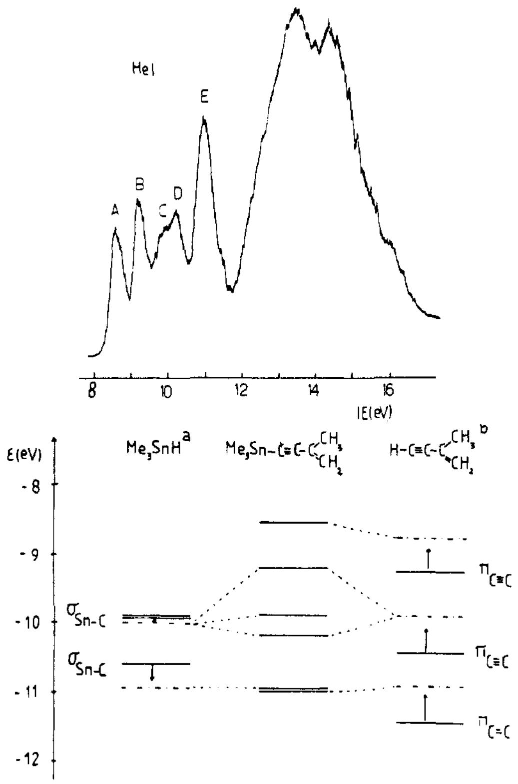

Figure 5. Gas-phase UP spectrum and correlation diagram of $Me_3SnC{\equiv}CC({=}CH_2)CH_3$ (see a and b in Figure 1).

therefore to be expected, as suggested in the figure. Following this scheme, the e′ antibonding and bonding combinations are associated with the A and C UPS bands respectively, and the e″ antibonding orbital is associated to band B, while the ionization from the e″ bonding combination contributes to the band envelope beyond 12 eV. Intensity considerations suggest that band C contains also both components related to the a_1-type Sn–C orbitals. On the other hand, the reduced splitting between these two components with respect to **3** is consistent with a weaker interaction due to the larger distance between two Me_3Sn moieties.

$Me_3SnC{\equiv}CC({=}CH_2)CH_3$ (5). In Figure 5 are shown the UP spectrum and the MO scheme for this low-symmetry molecule. For the parent molecule $HC{\equiv}CC({=}CH_2)CH_3$[21] the first and third highest MOs are the antibonding and bonding combinations of the π orbitals of the triple and double bonds, while the second MO is a pure $\pi_{C\equiv C}$ orbital. All these levels can interact with the σ_{Sn-C} orbitals. In the figure the most significant contributions to the various MOs are shown. Following this scheme, band A of the spectrum corresponds to a nearly pure π orbital mainly localized on the C≡C triple bond, with a contribution from the C═C double bond; bands B and D are related to the antibonding and bonding combinations, respectively, between the pure $\pi_{C\equiv C}$ orbital and the σ_{Sn-C} orbital; band C arises from the ionization from a σ_{Sn-C} level pratically not interacting with the π orbitals; band E, of intensity approximately twice that of the preceding bands, accounts for two ionization processes, one from a σ_{Sn-C} orbital and the other one from the π orbital of predominant $\pi_{C=C}$ character with admixture of the $\pi_{C\equiv C}$ orbital.

Comparison with ^{13}C and ^{119}Sn NMR Data. The calculated $C_{\alpha,\beta}$ atomic charges show an increase in the negative charge at both alkynyl carbon atoms. the $\delta(^{13}C_{\alpha,\beta})$ and, in particular, the $\Delta(^{13}C)$ values (Table VI) clearly indicate that there is no simple relationship between charge and the ^{13}C nuclear magnetic shielding.

The ^{13}C nuclear magnetic shielding of alkynyl carbon atoms in alkynes XC≡CY is best understood considering the tensorial components of the nuclear screening constant.[24,25] The most shielded direction will be along the

---

(24) Mehring, M. "Principles of High Resolution NMR in Solids", Springer-Verlag: Berlin, 1983; p 233 ff.

Table VI. ^{13}C and ^{119}Sn NMR Data[a] of the Alkynylstannanes

	$\delta(^{13}C_\alpha)$	$\Delta(^{13}C_\alpha)^b$	$\delta(^{13}C_\beta)$	$\Delta(^{13}C_\beta)^b$	$\delta(^{13}C_{SnCH_{2/3}})$	$\delta(^{119}Sn)$
$Et_3SnC_\alpha{\equiv}C_\beta H$	87.0 (344.2)	+14.7	97.6 (64.7)	+25.3	2.4 (390.6)	−56.5
$Me_3SnC{\equiv}CMe$	81.1 (502.9)	+13.5	105.7 (107.4)	+25.6	−8.2 (404.1)	−73.8
$Me_3SnC{\equiv}CSnMe_3$	115.5 (405.6)	+18.8	115.5 (48.3)	+26.8	−8.0 (400.7)	−80.9
$Me_3SnC{\equiv}CC{\equiv}CSnMe_3$[c]	83.9 (391.0)	*d*	93.3 (88.0)	*d*	−8.1 (404.5)	−61.5
$Me_3SnC{\equiv}CC(Me){=}CH_2$	92.1 (446.0)	+15.3	110.7 (91.6)	+25.6	−8.0 (405.6)	−67.0

[a] $\delta(^{13}C)$ and $\delta(^{119}Sn)$ relative to external Me_4Si and Me_4Sn, respectively; in C_6D_6. Data taken from ref 8d if not noted otherwise. [b] $\Delta(^{13}C) = \delta(^{13}C(SnC{\equiv}C)) - \delta(^{13}C(HC{\equiv}C))$. [c] Reference 8c. [d] $HC{\equiv}CC{\equiv}CSnMe_3$ has not been studied.

C≡C axis since there is no net paramagnetic circulation about the C_∞ or D_∞ axis. This situation reminds one of the behavior of the free atom in an external magnetic field. However, paramagnetic circulations of the type $\sigma \leftrightarrow \pi^*$ arising at the ≡CX and ≡CY bonds affect the nuclear shielding as well. Deshielding results in general if there are lone electron pairs at one or both nuclei forming the linear unit (e.g., $-C{\equiv}N|$, $|C{\equiv}N|^-$, N_2, F_2, etc.). Therefore, any polar ≡CX or ≡CY bond with excess negative charge at the alkynyl carbon atom is expected to produce a deshielding effect for the alkynyl ^{13}C nuclei. This situation is found in the alkynylstannanes, and the interpretation of the trends in the ^{13}C values is corroborated by the UPS data and the MO calculations.

Similarly, the fairly small computed overlap populations in the $Sn-C_\alpha$ bond (0.39 and 0.44 e^-) agrees with the behavior of the coupling constants $^1J(^{119}Sn^{13}C)$ (Table VI). These are considerably smaller in absolute magnitude than expected for the formal state of hybridization of carbon and tin. Also the fairly large overlap population calculated for the $Sn-CH_3$ or $Sn-C_2H_5$ bonds (0.7 and 0.69 e^-) is in line with the increase in $|^1J(^{119}Sn^{13}C)|$ with respect to tetraalkyl- or trialkylalkenylstannanes.[7,8,26,27]

The analysis of the overlap populations (Tables IV and V) indicates a larger $C_\alpha{\equiv}C_\beta$ overlap population (1.95 and 2.06 e^-) with respect to acetylene (1.79 e^-). This shows that the electron-releasing effect of the SnR_3 group does not involve interactions with the $\pi^*_{C\equiv C}$ orbitals. However, the experimental coupling constants $^1J(^{13}C{\equiv}^{13}C)$[7,8b,c,26,28] in alkynylstannanes at first glance indicate a very weak C≡C bond. This apparent inconsistency is explained by considering the nature of the $\sigma_{Sn-C\alpha}$ bond in the same way as that for the interpretation of the $\delta(^{13}C_{\alpha,\beta})$ values. The strongly polarized σ_{Sn-C_α} bond gives rise to negative contributions to the contact energy term leading to a decrease in the magnitude of $^1J(^{13}C{\equiv}^{13}C)$ irrespective of the $C_\alpha{\equiv}C_\beta$ overlap population.[7,26]

The ^{119}Sn nuclear shielding deserves a mention. There is an increase in the shielding of the ^{119}Sn nuclei if a sp^2 or sp-hybridised carbon atom is attached to tin.[8,27,29] In the latter case, in general, the shielding effect is greater. Assuming the dominance of the local paramagnetic term σ_p^{loc}, the ^{119}Sn nuclear shielding in tetraorganotin compounds with a tin coordination number of 4 depends mainly on paramagnetic currents arising at σ_{Sn-C} bonds. In trialkyltin compounds R_3SnX the electron-withdrawing effect of X (increase of σ_p^{loc}) may be compensated by σ/π interactions. These are, for steric and electronic reasons, particularly effective for X = alkynyl (with respect to X = vinyl, phenyl, etc.).

Final Remarks

The joint analysis of the experimental and theoretical data on this class of molecules revealed a very extensive mixing between the σ_{Sn-C} and the $\pi_{C\equiv C}$ orbitals. Also the important role played by the substituents in determining the extent and the mechanism of such a conjugation was pointed out. The UPS data are in agreement with NMR parameters. The trends observed for the chemical shifts $\delta(^{13}C)$ and the coupling constants $^1J(^{119}Sn^{13}C)$, $^1J(^{13}C{\equiv}^{13}C)$ are in agreement with the results of the MO calculations. Furthermore, the present study represents a test for the ability of the pseudopotential "ab initio" method to reproduce well the photoelectron ionization energies and to provide a nonempirical description of the electronic structure of molecules containing heavy atoms.

Acknowledgment. We wish to thank Dr. J. P. Daudey (Toulouse) for a copy of the PSHONDO code. This work is part of the national research project on gas-phase UPS sponsored by the Italian Ministry of Public Education.

Registry No. 1, 994-39-8; 2, 1692-19-9; 3, 2117-50-2; 4, 40762-69-4; 5, 1692-21-3; $Me_3SnC{\equiv}CH$, 1112-00-1.

---

(25) (a) Zilm, K. W.; Conley, R. T.; Grant, D. M.; Michl, J. *J. Am. Chem. Soc.* **1980**, *102*, 6672. (b) Diehl, P.; Moza, F. *J. Magn. Reson.* **1983**, *54*, 372.

(26) Wrackmeyer, B. *Spectrosc. Int. J.* **1982**, *1*, 201.

(27) Wrackmeyer, B. *Annu. Rep. NMR Spectrosc.*, in press.

(28) Kamienska-Trela, K. *J. Organomet. Chem.* **1978**, *159*, 15.

(29) Smith, P. J.; Tupcianskas, A. P. *Annu. Rep. NMR Spectrosc.* **1978**, *8*, 291.